

# Requirement for the zebrafish mid-hindbrain boundary in midbrain polarisation, mapping and confinement of the retinotectal projection\*

Alexander Picker<sup>1</sup>, Caroline Brennan<sup>2</sup>, Frank Reifers<sup>1</sup>, Jonathan D. W. Clarke<sup>2</sup>, Nigel Holder<sup>2</sup> and Michael Brand<sup>1,‡</sup>

<sup>1</sup>Department of Neurobiology, University of Heidelberg, Im Neuenheimer Feld 364, D-69120 Heidelberg, Germany

<sup>2</sup>Department of Anatomy and Developmental Biology, University College London, Gower Street, London WC1E 6BT, UK

\*This paper is dedicated to the memory of our friend and colleague Nigel Holder, who unexpectedly died while this manuscript was in preparation. He will be greatly missed

‡Author for correspondence (e-mail: brand@sun0.urz.uni-heidelberg.de)

Accepted 12 April; published on WWW 7 June 1999

## SUMMARY

The organizer at the midbrain-hindbrain boundary (MHB organizer) has been proposed to induce and polarize the midbrain during development. We investigate the requirement for the MHB organizer in *acerebellar* mutants, which lack a MHB and cerebellum, but retain a tectum, and are mutant for *fgf8*, a candidate inducer and polarizer. We examine the retinotectal projection in the mutants to assay polarity in the tectum. In mutant tecta, retinal ganglion cell (RGC) axons form overlapping termination fields, especially in the ventral tectum, and along both the anterior-posterior and dorsal-ventral axis of the tectum, consistent with a MHB requirement in generating midbrain polarity. However, polarity is not completely lost in the mutant tecta, in spite of the absence of the MHB. Moreover, graded expression of the ephrin family ligand Ephrin-A5b is eliminated, whereas Ephrin-A2 and Ephrin-A5a expression

is leveled in *acerebellar* mutant tecta, showing that ephrins are differentially affected by the absence of the MHB. Some RGC axons overshoot beyond the mutant tectum, suggesting that the MHB also serves a barrier function for axonal growth. By transplanting whole eye primordia, we show that mapping defects and overshooting largely, but not exclusively, depend on tectal, but not retinal genotype, and thus demonstrate an independent function for Fgf8 in retinal development. The MHB organizer, possibly via Fgf8 itself, is thus required for midbrain polarisation and for restricting axonal growth, but other cell populations may also influence midbrain polarity.

Key words: *Fgf8*, *Fgf*, *acerebellar*, Midbrain, Hindbrain, Midbrain-hindbrain boundary, Organizer, Zebrafish, *Danio rerio*, Retinotectal map, Engrailed, Eph family, Ephrin, Retina, Tectum

## INTRODUCTION

Establishment of cell type diversity in the vertebrate neural plate requires an interplay between intrinsic and extrinsic molecular mechanisms, mediated by transcription factors and secreted patterning molecules (review: Lumsden and Krumlauf, 1996). In the embryonic midbrain, these mechanisms cause different cell types to arise at precise anterior-posterior and dorsal-ventral positions. In addition, cells of a given type often show a rostrocaudal gradient of cytodifferentiation, particularly in the midbrain tectum (La Vail and Hild, 1971), where they receive spatially ordered afferent inputs from the retinal ganglion cells (RGCs) and thereby form a retinotopic map (review: Udin and Fawcett, 1988; Holt and Harris, 1993; O'Leary et al., 1999). At the molecular level, midbrain polarity is reflected in the graded distribution of the Engrailed (*En*) homeobox transcription factors (Martinez and Alvarado-Mallart, 1990; Davis et al., 1991; Itasaki et al., 1991), and of *ephrin-A2* (*ELF-1*) and *ephrin-A5* (*RAGS/AL-1*), two glycosylphosphatidylinositol (GPI)-linked ligands for Eph

family receptor tyrosine kinases (Cheng and Flanagan, 1994; Drescher et al., 1995). Via complementary gradients of tectal ligands and their receptors on ingrowing RGC axons, ephrins and their Eph receptors are thought to mediate the retinotopically organized projections of RGCs to their postsynaptic target cells in the tectum (reviews: Rétaux and Harris, 1996; Orioli and Klein, 1997; Flanagan and Vanderhaeghen, 1998; O'Leary et al., 1999). Misexpression of *En-1* or *En-2* in chick tecta suggest that they function upstream of the Ephrins (Logan et al., 1996; Friedman and O'Leary, 1996; Rétaux and Harris, 1996).

The molecular mechanisms which set up the graded distribution of these molecules are not known, but appear to be related to the initial formation of midbrain polarity. Tectum rotation experiments previously suggested that polarity becomes established prior to actual ingrowth of axons into the tectum, due to influences from adjacent cell populations (Nakamura et al., 1994). Two candidate cell populations located adjacent to the developing midbrain are at the forebrain-midbrain boundary (Chung and Cooke, 1978) and

the midbrain-hindbrain boundary (MHB). When MHB tissue is transplanted to ectopic locations in the posterior forebrain, it can induce midbrain differentiation in surrounding host cells, which in turn can act as targets for RGCs. In addition to its inductive abilities, the MHB tissue also exerts a polarizing influence on the induced tissue: for instance, the induced host cells express Engrailed antigens at levels that decrease with distance from the graft. We will refer to this polarizing activity as *midbrain polarizing activity*, or MPA. The effects of transplanted MHB tissue can be mimicked by inserting beads soaked with Fgf8 (or Fgf4) protein (Crossley et al., 1996; Shamim et al., 1999), two secreted members of the fibroblast growth factor family, which are expressed in MHB tissue, but not by the adjacent tectum (Crossley and Martin, 1995; Reifers et al., 1998; Shamim et al., 1999; unpublished observations). Together with the results of misexpression experiments of Fgf8 in mice (Lee et al., 1997), this raises the possibility that Fgf8 and/or Fgf4 may correspond to the midbrain inducing activity and/or the MPA. While these experiments establish that MHB tissue or Fgfs are able to polarize in ectopic sites, the requirement for the MHB organizer or for Fgf8 in midbrain polarisation has not been examined.

Zebrafish embryos homozygous for the recessive *acerebellar* (*ace*) mutation lack the morphogenetic constriction (isthmus constriction), which we here refer to as MHB, between the midbrain and rhombomere one, whereas the adjacent midbrain is still present (Brand et al., 1996; Reifers et al., 1998; Brand, 1998 and unpublished observations). *fgf8* and *wnt1* expression, normally seen in a subset of the MHB cells which may mediate its organizing potential, is absent in *acerebellar* mutants, indicating that the MHB organizer itself is absent in *acerebellar* mutants. We have previously shown that *acerebellar* is a loss-of-function mutant of *fgf8*, and argued that Fgf8 functions during maintenance, rather than initial induction, of midbrain development (Reifers et al., 1998). In particular, the observation that Fgf8 is required to maintain expression of the three zebrafish engrailed genes (*eng1* to *eng3*), *wnt1* and other genes suggests that Fgf8 might be a component of the MPA emanating from the MHB.

Here, we use the retinotectal system as a fine-grained readout to assess midbrain polarity in *acerebellar* mutant embryos. The tectum is the largest retinofugal target of RGC axons in zebrafish, and as in other vertebrates, the projection is retinotopically organized, such that neighbouring RGCs in the retina connect to neighbouring tectal target cells (Stuermer, 1988; Burrill and Easter, 1994). During embryonic development, RGCs grow through the optic nerve, chiasm and optic tract to reach the tectum, where they synapse at the correct retinotopic target site. Initial growth to the target site is direct (Kaethner and Stuermer, 1992) and does not involve competition for target area or electrical activity (Harris, 1980; Stuermer et al., 1990; Kaethner and Stuermer, 1994). Within the tectum, three zebrafish ephrins, *ephrin-A5a* and *ephrin-A5b*, both related to mammalian *ephrin-A5* (*RAGS/AL-1*) and *ephrin-A2*, related to murine *ephrin-A2* (*Elf-1*) are distributed in increasing anterior to posterior gradients. Consistent with a function for these molecules in map formation, *in vitro* stripe assays (Walter et al., 1987) have shown that the zebrafish ephrins repel both temporal (*Ephrin-A5b* and *Ephrin-A2*) and nasal axons (*Ephrin-A5b*; Brennan et al., 1997). Moreover, targeted inactivation of murine *ephrin-A5* leads to ectopic

termination of RGCs in the superior colliculus, and to overshooting projections into the inferior colliculus (Frisén et al., 1998).

By studying the midbrain of *acerebellar* mutants, we show here that the MHB is required for anterior-posterior polarization of the midbrain retinotectal map, to restrict growth of RGC axons to the tectum, and for graded expression of ephrin ligands in the midbrain neuroepithelium prior to axonal ingrowth. Since Fgf8 is mutated in *acerebellar*, Fgf8 itself might be involved in establishment of midbrain polarity. Unexpectedly, our results also suggest that Fgf8 is required for normal retinal patterning and dorsal-ventral polarization of the tectum.

## MATERIALS AND METHODS

### Fish maintenance

Zebrafish were raised and kept under standard laboratory conditions at 27°C (Westerfield, 1994, as described in Brand and Granato, 1999) and heterozygous carriers were identified by random intercrosses. To obtain homozygous mutants, carriers were crossed to each other. Embryos were incubated at 28.5°C in embryo medium with 0.2 mM PTU to prevent melanization and fixed according to hours of development and morphological staging criteria (Kimmel et al., 1995).

### Whole-mount *in situ*, immunocytochemistry and nomenclature

Whole-mount RNA *in situ* hybridisation (ISH; Reifers et al., 1998), receptor alkaline phosphatase staining with the chick EphA3/AP, zebrafish EphB4b/AP and Ephrin-A5b/AP fusion proteins on whole-mount embryos (Cheng and Flanagan, 1994; Brennan et al., 1997) and antibody stainings against acetylated tubulin (Macdonald et al., 1997) were described previously. Zebrafish *ephrin-A5a*, *-A5b* and *-A2* were previously designated *zEphL2*, *-L4* and *-L3*, respectively (Brennan et al., 1997). Probably due to a partial genome duplication (Postlethwait et al., 1998), *ephrin-A5a* and *ephrin-A5b* are two separate genes that are both related to mammalian *ephrin-A5*.

### RGC labelling

For RGC axon tracing, larvae were fixed in 4% paraformaldehyde in PBS at 4°C over night, embedded in 2% LMP agarose (GIBCO BRL) on slides and labelled by inserting glass needles covered with either molten DiI or DiO (Molecular Probes D-282, D-275) into the retina. After overnight storage at room temperature in a dark moist chamber, larval brains were dissected and further processed for microscopy. Whole-eye-fills were done by pressure injection of saturated DiI or DiO solutions in chloroform into the eyes of fixed larvae. To determine their morphology, larval brains were dissected using watchmaker forceps and stained for DNA with 0.5 µM SYTOX (Molecular Probes S-7020) in PBS for at least 24 hours at room temperature. Brain morphology, retinotectal projection and ephrin RNA expression were analysed on fluorescent preparations with a LEITZ DM IRB confocal microscope, equipped with a TCS 4D Argon/Krypton laser and SCANware 5 software.

### Quantification of ligand expression

*In situ* hybridisations on high pec stage embryos (42–44 hours) were performed as described previously (Xu et al., 1994) except that embryos were developed after ISH with FastRed (Boehringer) as a fluorescent substrate. Thick sections, which bisected the tectum along the anterior-posterior axis in the direction of entry of the axons to the tectum, were cut using a sharpened tungsten needle and mounted for confocal analysis. The gradient along the anterior-posterior tectal axis

at approximately the mid-point of each tectum was determined (mean of 5 scans) for at least ten mutant embryos and ten siblings for each probe. Confocal data were quantitated using NIH image and are presented in graphical form.

### Optic vesicle transplantation

Fertilized eggs, to be used as donors, were fluorescently labelled by intracellular pressure injection of 10% tetramethylrhodamedextran, 10,000 MW (Molecular Probes D-1817) in 0.25 M KCl and after 50% epiboly raised together with unlabelled host at 18°C to the 8-10 somite stage. For grafting, live embryos were embedded in 1.2% ultra pure LMP agarose in Ringer at 42°C (GIBCO) and operated in sterile zebrafish Ringer (Westerfield, 1994) in a Petri dish cover under a dissecting microscope. To access the optic vesicles, the epidermis was locally destroyed with a drop of light mineral oil (Sigma M-8410) and removed. Optic vesicles were grafted with electrolytically sharpened tungsten tools. Within the first hour after transplantation, when healing was complete, the embryos were removed from the agarose and raised under standard conditions in sterile Ringer until day 6. One day after transplantation, embryos were scored for position, orientation and vitality of the graft, using a fluorescence microscope.

## RESULTS

### Phenotypic variability, tectal morphology and retinofugal targets in *ace* larvae

We examined the retinotectal projection of *ace* mutant larvae after its establishment on day 6 of development, although similar defects to those described here are also apparent on day 3, albeit in a much smaller tectum (unpublished results). At day 3 of development, the mutant larvae were divided into two classes of different phenotypic strength: type A larvae (78%,  $n=235$ ) show little overall malformations, whereas type B larvae (22%) are overall retarded compared to the wild type of the same age, probably as a secondary consequence of variably abnormal circulation (Brand et al., 1996; Fig. 1A,B). We examined the overall morphology of wild-type and mutant tecta in whole-mounted brains stained with the fluorescent DNA stain Sytox (Fig. 1C-G). As described previously, the cerebellum is missing in the mutants (Reifers et al., 1998). In type A larvae, the tectum is slightly altered in its shape, but not affected in its anterior-posterior length along the dorsal midline. Since the brain of type B larvae is overall reduced in size (Fig. 1E), tectal defects in type B larvae are

likely to be influenced by secondary effects. Our subsequent analysis therefore focusses on type A larvae, although type B individuals show similar retinotectal defects (data not shown). We find that the termination zone of RGC axons in the tectum (neuropil) of type A individuals is reduced in size and located more posteriorly (Fig. 1F,G), as confirmed by anterograde labelling of the retinofugal projection with DiI, which also reveals that axons enter the tectum via abnormal brachia (Fig. 1H,I). In addition, the arborization field AF-7 at the diencephalic-mesencephalic boundary (Burrill and Easter, 1994) is enlarged in 8 of 11 mutants, and the space between AF-7 and the anterior neuropil margin is wider in 10 of 11 mutants examined. We believe that this phenotype reflects a more anterior character of the tectum in *ace* mutants (see below).

### Mapping defects of RGC axons on the optic tectum

To assess the size and position of RGC axon termination fields on the tectum, we labelled subpopulations of RGCs anterogradely with DiI or DiO and found a pronounced, but partial disruption of the retinotectal map in *ace* tecta compared to the wild type. The terminations of wild-type RGC axons form an inverted map on the tectum, such that dorsal and ventral RGCs project to the ventral and dorsal tectum, respectively, and nasal and temporal RGCs project to the posterior and anterior tectum, respectively. Whereas the anterior-posterior position at which ventrotemporal RGC axons terminate in the

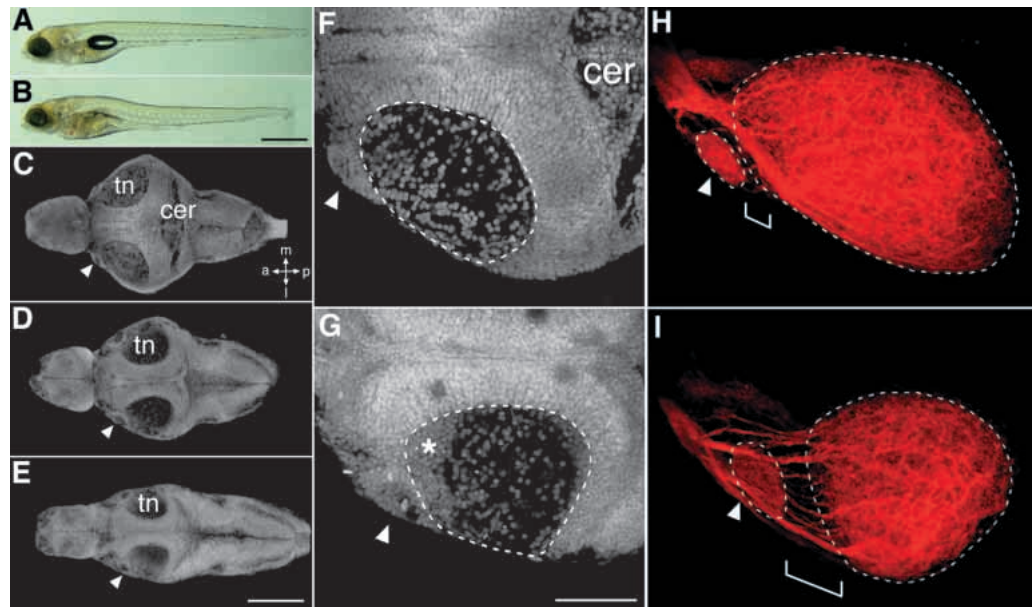
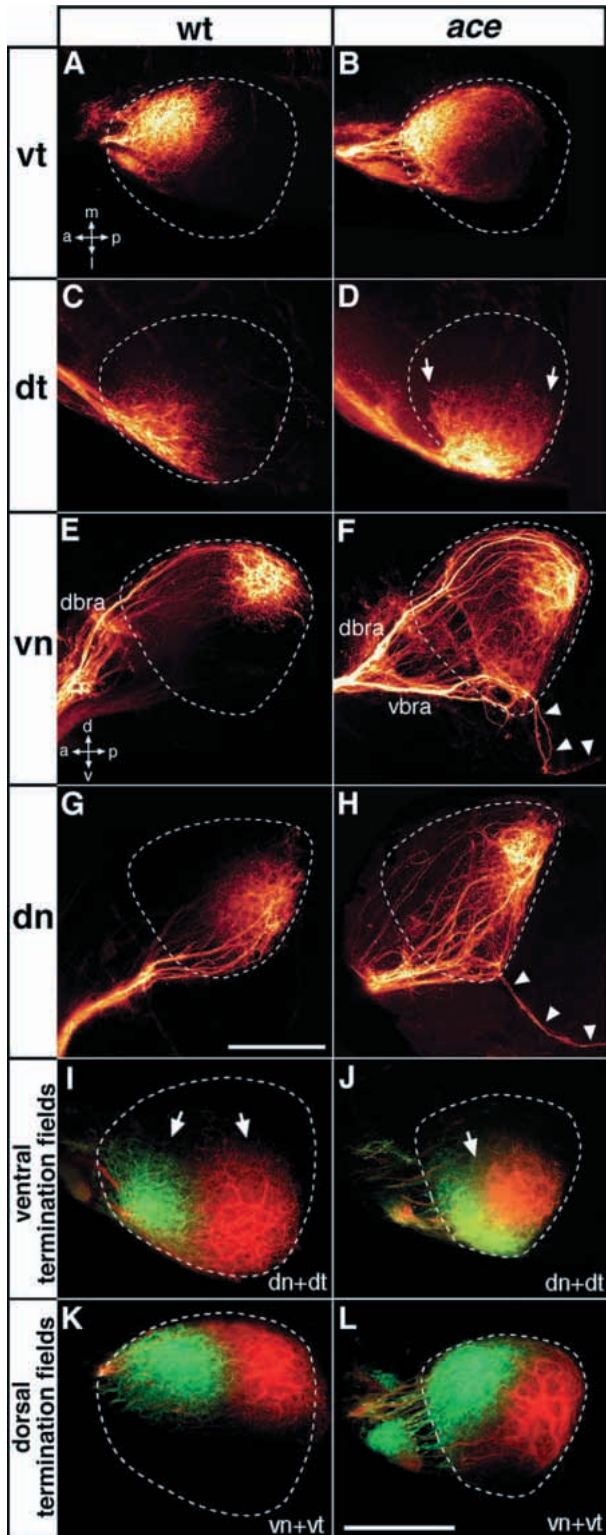


**Fig. 1.** Larval phenotype and midbrain morphology of wild type and *ace* mutants at day 6. (A,B) Lateral view of (A) a wild type and (B) a type A *ace* larva. (C,D) Dorsal view confocal scans of (C) a whole-brain-preparation of a wild type, (D) a type A *ace* larva and (E) a type B *ace* larva stained with the fluorescent nuclear dye Sytox. Mutant type A larvae show a smaller tectal neuropil and have no cerebellum. Type B larvae show overall altered brain morphology. (F,G) Dorsal view of a (F) left hemitectum in a wild-type larva and (G) a type A mutant larva; the neuropil is outlined. The mutant tectum is slightly smaller. Due to the reduced neuropil size, some ventral nuclei (asterisk) give the impression that they lie within the neuropil, because of the projection of the confocal sections; compare also to (D). (H,I) DiI labelling of RGC projections to the left hemitectum of (H) a wild type and (I) *acerebellar* mutant. In the mutant, the tectal neuropil (large outlined area) is reduced in size and located more posteriorly, and axons enter the tectum via abnormal brachia. The pretecal arborization field AF-7 (arrowheads; see also arrowheads in C-G) and the distance between AF-7 and the tectal neuropil (brackets) is enlarged. Orientation as indicated in C: a, anterior; cer, cerebellum; l, lateral; m, medial; p, posterior; tn, tectal neuropil. Scale bars, (A,B) 700  $\mu$ m; (C-E) 150  $\mu$ m; (F,G) 60  $\mu$ m and (H,I) 40  $\mu$ m.



dorsoanterior neuropil is almost correct (Fig. 2A,B), the tectal termination field of dorsotemporal RGCs is expanded from its normal ventroanterior position throughout the posterior neuropil in 12 of 17 *ace* larvae (Fig. 2C,D). Importantly, both temporal RGC subpopulations have partially delocalized projection fields along the dorsal-ventral axis of the tectum (Fig. 2B,D): dorsotemporal RGCs misproject to the dorsal neuropil

**Fig. 2.** Topographic mapping of RGC axon projections is altered in *ace* mutants. Dorsal (A–D) and lateral (E–H) views of the tectal termination fields of wild type and *ace* mutants. The tectal neuropil is outlined in all panels. (A,B) Ventrotemporal RGC axons in wild-type larvae terminate on the dorsoanterior tectum. In *ace* mutants the termination field expands mainly to the ventral neuropil, as confirmed by the double labellings (K,L). (C,D) Ganglion cell axons from the dorsotemporal retina terminate in the ventroanterior tectum in the wild type, but are delocalized throughout the posterior and dorsal tectal neuropil in the mutant (arrows), as confirmed by the double labellings (I,J). (E,F) Ventronasal RGC axons in the wild type project to the dorsoposterior tectal termination field via the dorsal brachium of the optic tract (dbra). In the mutant this termination field is mainly delocalized towards the ventral neuropil. Note the overshooting projection (arrowheads). Axons also misproject through the ventral brachium (vbra) and intermediate fascicles (see text). (G,H) Dorsonasal RGCs terminate in the ventroposterior tectum in the wild type, but spread to dorsoposterior neuropil in the mutant. Note the posteriorly overshooting axons (arrowheads) in the mutant, which are most frequently seen in dorsonasal RGCs. (I–L) Ventral tectal termination fields overlap in *ace*. Double labelling of the temporal RGCs in green and nasal RGCs in red. The two ventral termination fields are separated in the wild type (arrows in J) but strongly, though not completely, overlap along the anterior–posterior axis in the mutant (arrow in J). The dorsal termination fields are non-overlapping in the wild type (K) and in *ace* (L). The mutant shows delocalization of all termination fields along the dorsal–ventral axis of the tectum. a, anterior; d, dorsal; dn, dorsonasal RGCs; dt, dorsotemporal RGCs; l, lateral; m, medial; v, ventral; vn, ventronasal RGCs; vt, ventrotemporal RGCs. Scale bar, 75  $\mu$ m.

in 13 of 17, and ventrotemporal RGCs to the ventral neuropil in 12 of 24 mutant larvae.

Whereas the termination fields of especially dorsotemporal RGCs are clearly delocalized along the anterior–posterior axis, nasal RGCs are predominately affected along the dorsal–ventral axis and appear to follow aberrant routes through the tectum. Whereas wild-type ventronasal RGCs terminate only in the dorsoposterior neuropil, ectopic terminations are also found in the ventroposterior tectum in 12 of 17 mutants (Fig. 2E,F), independently of the brachium they have chosen (Table 1, see below). Similarly, the dorsonasal RGCs, which in the wild-type terminate in the ventroposterior region of the neuropil, in 14 of 19 *ace* mutants form ectopic axon terminations in the dorsoposterior tectal neuropil (Fig. 2G,H).

To further investigate the relative localization of tectal termination fields in *ace* mutants, we performed double labellings of RGCs axons from neighbouring quadrants of the retina. In the wild type, RGCs from the dorsonasal and dorsotemporal retinal quadrants form non-overlapping tectal termination fields in the ventroanterior and ventroposterior neuropil (Fig. 2I). In *ace* mutants, the termination fields of these two RGC populations overlap in a medial position along the anterior–posterior axis of the neuropil (Fig. 2J). In contrast, the anterior–posterior extent of the termination fields in the dorsal tectum of *ace* mutants is similar to the wild type, and not overlapping, despite a prominent dorsal–ventral delocalization (Fig. 2K,L). In summary, the exact 1:1-representation of retinal positions on the tectum is lost in *ace* for all four analysed retinal quadrants due to mapping errors along both the anterior–posterior and dorsal–ventral axis of the optic tectum. The changes in anterior–posterior polarity are more pronounced in the ventral than the dorsal tectum.

### Posterior overshooting of RGC axons in *ace*

In addition to mapping errors we find that all RGC subpopulations show 'overshooting' axonal projections beyond the posterior border of the tectal neuropil into the hindbrain (Fig. 2F,H). Overshooting RGC axons exit the neuropil preferentially at the ventroposterior margin of the tectal neuropil in 16 of 18 mutants, and only rarely in dorsoposterior regions of the neuropil (2 of 18 mutants); here, filopodia sometimes abnormally explore beyond the neuropil, although they are not elaborated into complete overshooting projections (not shown). Overshooting is most frequent for the dorsonasal RGC axons (12 of 19 mutants, Fig. 2H), which normally project to the ventroposterior part of the neuropil and thus are spatially closest to the favoured exit point. Ventronasal RGCs overshoot in 8 of 17 (Fig. 2F), dorsotemporal RGCs in 5 of 17 and ventrotemporal RGCs in 5 of 24 analysed mutant larvae. These findings suggest that a repulsive property of the MHB might be absent in *acerebellar* mutants. Interestingly, the trochlear nerve, which normally grows through the posterior, cerebellar part of the MHB, abnormally invades the tectal area in *ace* mutants (Fig. 3J,K), suggesting that the repulsive property of the MHB is not specific for RGC axons.

### Sorting of RGC axons in the brachia of the optic tract and dorsal-ventral mapping

Shortly before reaching the anterior border of the tectal neuropil the optic tract normally separates into two fascicles, the dorsal and ventral brachium. RGC axons from the ventral

retina are invariably sorted into the dorsal brachium and dorsal RGC axons into the ventral brachium (Stuermer, 1988). This sorting is variably abnormal in *ace* larvae. For all four retinal quadrants, many larvae show axonal projections via the wrong brachium and ectopic tracts at intermediate dorsal-ventral positions along the anterior boundary of the neuropil (e.g. Fig. 2F). Since brachial missorting might cause the abnormal dorsal-ventral topography of termination fields on the *ace* tectum, we investigated whether dorsal-ventral errors are also seen in larvae with normal brachial sorting (Table 1). In mutant individuals where temporal RGC axons enter the tectum through their normal brachium, dorsal-ventral mapping mistakes are only rarely seen (2 of 12, respectively 1 of 11 larvae examined). Conversely, even if nasal RGC axons enter through their normal brachium, dorsal-ventral delocalization nevertheless occurs in most individuals, and is therefore probably due to mapping errors in the posterior tectum (9 of 11, respectively 11 of 12 larvae examined).

### Ephrin expression is anteriorized in the *ace* midbrain

To examine the molecular basis of the retinotectal defects in *ace*, we studied expression of *ephrin-A5a*, *ephrin-A5b* and *ephrin-A2*. mRNAs of all three ephrins are expressed in anterior to posterior increasing gradients in the midbrain and MHB of wild-type embryos at 24 and 48 hours (Fig. 3) at least until 84 hours, the latest stage we have examined (unpublished observations). The gradients of *ephrin-A5a* and *ephrin-A2*

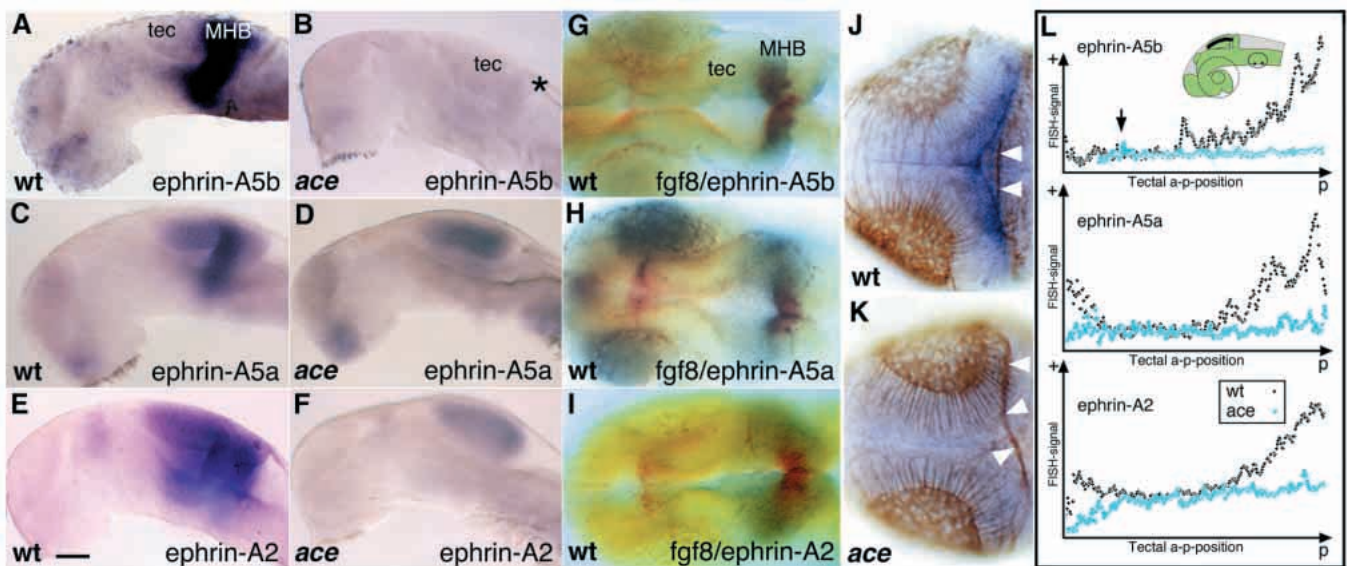


**Fig. 3.** Altered ephrin RNA expression in the *acerebellar* tectum. (A,C,E) Wild-type and (B,D,F) *ace* mutant embryos at 24 hours. Graded *ephrin-A5b* expression (A,B) is absent in the mutants, and *ephrin-A5a* (C,D) and *ephrin-A2* (E,F) expression is leveled along the anterior-posterior axis of the tectum in *ace*. The asterisk indicates the missing MHB. Double in situ hybridizations for *fgf8* (blue) and *ephrin-A5b* (red in G), *ephrin-A5a* (red in H) and *ephrin-A2* (red in I) in wild-type embryos at 44 hours, show expression of the ligands, which posteriorly overlaps with the MHB domain of *fgf8*. (J,K) Double labelings for acetylated tubulin (brown) and *ephrin-A5b* (purple) at 72 hours shows expression of *ephrin-A5b* in tectal cells posterior and posterior-medial to the tectal neuropil in the wild type (J), which is absent in *ace* (K). The trochlear nerve (arrowheads) abnormally projects into the posterior right hemitectum in *ace*. (L) Quantification of tectal ephrin gradients. RNA expression of the *ephrin-A5b*, *ephrin-A5a* and *ephrin-A2* genes at 24 hours forms an anterior to posterior increasing gradient in the wild type (black) which is reduced in the *ace* mutant (blue) to either no expression (*ephrin-A5b*) or a level of expression characteristic for anterior tectal position (*ephrin-A5a* and *ephrin-A2*). Values were determined by confocal scans of embryos processed for fluorescent in situ hybridization. Scaling of graph axes is arbitrary. Arrow marks diencephalic-mesencephalic boundary and inset shows trajectory of the confocal scan. (A-F) Lateral views with dorsal up and anterior to the left. (G-K) Dorsal views with anterior to the left. Scale bars 120  $\mu$ m (A-F), 50  $\mu$ m (G-I), 100  $\mu$ m (J,K). p, posterior; FISH-signal, relative intensity of fluorescent in situ hybridization signal; tec, tectum.

reach into the anterior tectum, whereas *ephrin-A5b* expression is confined to the posterior midbrain and MHB (Fig. 3; Brennan et al., 1997), where ephrin expression overlaps with *fgf8*-expressing cells (Fig. 3G-I). In *ace* mutants, expression of *ephrin-A5b* is reduced at the MHB from the 16 somite stage onwards and is not detectable beyond 24 hours (Fig. 3A,B), whereas *ephrin-A5a* and *ephrin-A2* are still expressed at low levels, but at an even distribution compared to the wild-type tecta (Fig. 3C-F). We quantitated relative ephrin mRNA expression levels along the anterior-posterior axis of the tectum after fluorescent ISH at 42-44 hours, a stage directly prior to RGC axon ingrowth to the tectum (Fig. 3L). Whereas the graded distribution is clearly evident in wild-type tecta, the gradients are absent or flattened in the mutant tecta; in particular the expression of *ephrin-A2* and *ephrin-A5a* appear reduced to a level characteristic for anterior tectal areas.

To ensure that alterations in RNA levels reflected changes in protein distribution, we used an EphA3/AP-fusion protein that recognizes all known ephrin-A proteins (Brennan et al., 1997). Ephrin-A protein level is strongly reduced in mutant tecta at 24 and 44 hours, and the normally graded distribution of the ephrins again appears flattened along the anterior-posterior (Fig. 4A-H) and, notably, also the dorsal-ventral axis in *ace* mutants (Fig. 4I,J). The residual protein appears somewhat concentrated in the dorsoposterior tectum, especially at 44 hours (Fig. 4E-H). In summary, in the wild type, the shape and steepness of the gradient differs with the ligand considered. In *ace* mutants, ephrin mRNA and protein expression is either eliminated or flattened in the tectum as a consequence of the missing MHB, but a minor amount is still detectable in the dorsoposterior tectum.

### Abnormal mapping and overshooting are due to brain genotype

Apart from the MHB, *Fgf8* is also expressed in the retina and optic stalk (Reifers et al., 1998), suggesting that the retinotectal projection phenotype of *ace* could be partially due to autonomous defects in RGCs. To distinguish the contributions of *Fgf8* function to retinal and tectal patterning, we performed optic vesicle transplantation experiments to combine eyes with a brain of different genotype in one chimaeric individual, using a novel technique developed by Chi-Bin Chien (personal communication). Optic vesicles were transplanted at the 8-10 somite stage from fluorescently labelled donor embryos into unlabelled hosts, from which the optic vesicle had been removed on one side (Fig. 5A). The unoperated contralateral side served as an internal control, and donors were raised to determine the genotype of the transplant. Transplanted eye vesicles heal in smoothly about 1 hour after transplantation, and by 30 hours of development, prior to RGC axon outgrowth from the eye, transplanted and unoperated eyes are indistinguishable, indicating that healing is complete (Fig. 5B-F). After 6 days of development the chimaeric larvae were analysed for the topography of the

**Table 1. Brachial missorting and dorsal-ventral delocalization**

Genotype	RGC population	Brachium	Number of larvae with dorsal-ventrally delocalized termination fields*
wt	vt/vn	dorsal	0 (19)
wt	dt/dn	ventral	0 (19)
<i>ace</i> ‡	vt	dorsal	2 (12)
<i>ace</i>	vn	dorsal	9 (11)
<i>ace</i>	dt	ventral	1 (11)
<i>ace</i>	dn	ventral	10 (12)

\*Total number of larvae tested in brackets.

‡For the mutant only individuals with normal brachial sorting are given.

Dorsal-ventral delocalization of RGC termination fields was examined in those *ace* larvae where RGC axons had entered the tectum through their normal brachium. No delocalization is observed in wild-type larvae. Delocalization of ventronasal and dorsonasal RGC target fields in the posterior tectum is seen in spite of normal brachial sorting. In contrast, dorsal-ventral delocalization of temporal RGC termination fields is only rarely seen in mutants with normal brachial sorting. dn, dorsonasal; dt, dorsotemporal; vn, ventronasal; vt, ventrotemporal; wt, wild type.

retinotectal projection between the donor eye and the host optic tectum by anterograde dye-labelling.

In control transplantations of wild-type eyes into a wild-type host, the manipulation does not affect the topographic order of the retinotectal map (Fig. 6A-C; Table 2). Similarly, control transplantations of *ace* eyes into *ace* hosts result in the same altered topography of the retinotectal projection, overshooting, brachial missorting and pathfinding errors as in non-manipulated *ace* larvae (Fig. 6D-F and not shown).

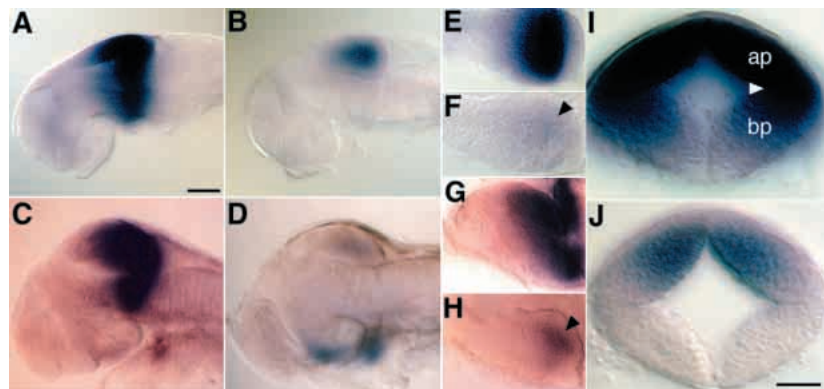
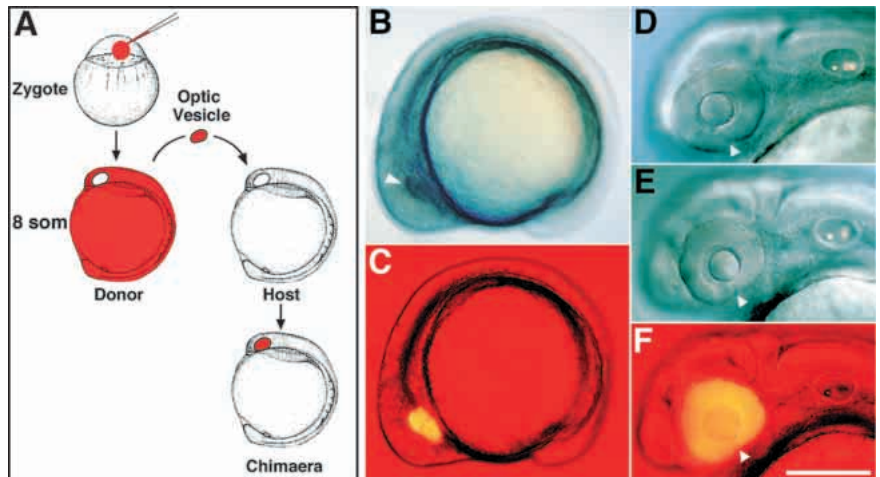


**Fig. 4.** Altered ephrin protein expression in the *acerebellar* tectum. Expression of ephrin-A proteins in the midbrain of wild type (A,C,E,G,I) and *ace* mutant embryos (B,D,F,H,J) detected by an EphA3/AP fusion protein. At 26 hours ephrin-A proteins form a steep anterior to posterior gradient of expression with a posterior border at the mid-hindbrain boundary in the wild type (A), whereas expression is reduced in the mutant (B). At 44 hours, the onset of RGC axon ingrowth into the tectum, a similar gradient is seen in the wild type (C) but in the mutant (D) protein expression is reduced. Flat mounts of left hemitecta from 26 hour (E,F) and 44 hour (G,H) embryos. Ephrin-A protein expression in the mutants is largely eliminated, but remnants are present in the dorsoposterior tectum (arrowheads). (I,J) Transverse sections at the level of the posterior midbrain at 26 hours in a wild-type embryo (I), showing dorsal-ventrally graded expression of ephrin-A proteins in the alar (ap) and basal plate (bp), which is reduced in the mutant (J). Arrowhead in I indicates the sulcus limitans. For A-H orientation is anterior to the left and dorsal up. For (I,J) dorsal is up. Scale bars (A-D) 50  $\mu$ m; (E-H) 40  $\mu$ m (I,J) is 30  $\mu$ m.

**Fig. 5.** Optic vesicle transplantation. (A) Schematic of the transplantation procedure. Optic vesicles of a fluorescently labelled donor are grafted to a non-fluorescent host to produce a chimaeric embryo. (B) Lateral bright-field image of 15-somite host, which received an optic vesicle graft (arrowhead). (C) Fluorescent image of the chimaera in B, showing the position and integration of the fluorescently labelled graft. (D) Non-operated left eye in the same chimaera at 30 hours. (E) Grafted eye on the right side of the same wild-type host as in D. Healing and integration of the graft is complete. The grafted eye is normally vascularized and positioned. (F) Fluorescent image of E, showing that the fluorescent signal is confined to the graft. In B-F anterior is to the left, dorsal is up, arrowheads indicate ventral position of the choroid fissure. Scale bar, 200  $\mu$ m (D-F) and 300  $\mu$ m (B,C).



Transplantation of wild-type eyes into *ace* hosts reproduces the aberrations in retinotectal topography of *ace* mutants (Fig. 6G-O): axon projections from the dorso-temporal and dorsonasal retina strongly overlap along the anterior-posterior axis of the ventral tectum and their termination fields are expanded along the dorsal-ventral axis (Fig. 6G-I; see also Fig. 3C), whereas mapping of the ventrotemporal and ventronasal RGCs is only affected along the dorso-ventral axis of the tectum (Fig. 6M-O; see also Fig. 3D). In addition, missorting in the optic tract, enlargement of AF-7 (not shown) and overshooting (Fig. 6J-L) are observed. In the reciprocal chimaeras, wild-type embryos with an *ace* eye, dorso-temporal axons terminate normally in the ventroanterior tectum and do not overshoot (Fig. 6P-R).

The above findings show that the defects in the chimaeras depend on the genotype of the brain. However, analysis of dorsonasal RGCs also demonstrates an autonomous requirement for *fgf8* in retinal development: dorsonasal axons that should only terminate in the ventroposterior tectum

additionally project to the ventroanterior tectum (Fig. 6P-R; Table 2). Posterior overshooting of RGC projections towards the hindbrain is not detectable.

In conclusion, the transplantation experiments show that disturbed mapping, overshooting and brachial missorting of the RGC axons in *ace* are mainly due to alterations in the *ace* brain (Fig. 7). Nevertheless, an autonomous function for *Fgf8* in retinal development is evident which requires further investigation.

## DISCUSSION

### The MHB is required to polarize the retinotectal map

Our study on the requirement of the MHB in *acerebellar/fgf8* mutants demonstrates a dual function: one, in generating polarity of the retinotectal map, and a second, in confining growth of RGC axons to the tectum at the posterior tectal margin (Fig. 7). Transplantation studies in chick have previously identified two potential sources for a midbrain polarising activity (MPA) which influences the graded distribution of the Engrailed transcription factors: (i) the diencephalic-mesencephalic boundary negatively influences Engrailed expression (Chung and Cooke, 1978; Itasaki and Nakamura, 1992), and (ii) the MHB organizer can activate Engrailed expression when placed ectopically (Gardner and Barald, 1991; Martinez et al., 1991). This is reflected in the topography of RGC projections: RGC axons are able to recognize ectopically formed tecta with some topographic specificity (Itasaki and Nakamura, 1992). The early requirement for murine En-1 in development of the midbrain primordium has so far precluded studying the tectum of these mutants directly (Wurst et al., 1994; Joyner, 1996); En-2 mutants appear to have no defects in midbrain development (Millen et al., 1994). However, misexpression of En-1 and En-2 in anterior chick tectum leads to upregulation of Ephrin ligands and avoidance by RGC axons (Logan et al., 1996; Friedman and O'Leary, 1996). These findings support a central role for the Engrailed gradient in controlling downstream properties in the midbrain tectum, which is generally confirmed for the zebrafish by our study. Expression of all three zebrafish *Engrailed* genes is lost specifically in the tectum and MHB during midsomitogenesis in *acerebellar* mutant embryos

**Table 2. Anterior-posterior retinotectal topography in chimaeras\***

Donor genotype	Host genotype	Delocalized dn+dt field	Delocalized vn+vt field	Duplicated dn field	Overshooting
wt	wt	0 (6)	0 (6)	0 (6)	0 (12)
<i>ace</i>	<i>ace</i>	7 (7)	0 (5)	0 (7)	7 (12)
wt	<i>ace</i>	6 (6)	0 (6)	0 (6)	10 (12)
<i>ace</i>	wt	0 (6)	0 (4)	5 (6)	0 (10)

Control transplantation of a wild-type optic vesicle to wild-type host results in a normal retinotectal projection with the described topography. Control transplantation of an *ace* optic vesicle to an *ace* host reproduces the *ace* projection phenotype. Transplantation of a wild-type optic vesicle to an *ace* host completely reproduces the *ace* phenotype, including delocalized and overlapping termination fields of dorsonasal and dorso-temporal RGC axons and axonal overshooting. As in *ace*, termination fields of ventronasal and ventrotemporal RGC axons are not overlapping in these chimaeras, but dorsal-ventral overlap is seen for all RGC subpopulations (not shown). Transplantation of an *ace* optic vesicle to a wild-type host results in a wild-type projection phenotype, with the exception of a duplicated termination field, which is formed by mutant dorsonasal RGC axons in the ventroanterior wild-type tectum. dn, dorsonasal RGC axons; dt, dorso-temporal RGC axons; vn, ventronasal RGC axons; vt, ventrotemporal RGC axons.

\*Topography of termination fields in chimaeras was not evaluated with respect to dorsal-ventral effects.

Total number of larvae tested are given in brackets

(Brand et al., 1996; Reifers et al., 1998). Our present results show that the tecta of *ace* mutants lack Ephrin-A5b ligand, and have more even, instead of graded, distribution of Ephrin-A5a and Ephrin-A2 ligand. In the ventral tectum, absence of ephrin ligands correlates with the severe anterior-posterior delocalization we observe for the projection fields of nasal and temporal RGCs. This is consistent with a functional requirement for the zebrafish ephrin-A5 and -A2 homologues in mediating mapping along the anterior-posterior axis of the tectum, as suggested previously on the basis of their distribution and in vitro activity (Brennan et al., 1997). However, anterior-posterior polarity is not completely lost in the ventral tectum, and is surprisingly normal in the dorsal tectum, in spite of the absence of the MHB and the severe reduction of graded ephrin expression. The weaker effect on the dorsal tectum may be due to the residual dorsoposterior Ephrin expression we have observed. Alternatively, axons could also respond to other graded, non-Ephrin molecules that are unaffected by the absence of the MHB (Rétaux and Harris, 1996). Residual midbrain polarity could for instance be due to the presence of other, unaffected cell populations in the mutants, such as the cells of the di-mesencephalic boundary (Chung and Cooke, 1978; Itasaki and Nakamura, 1992), or cells of the hindbrain which are not normally in touch with the midbrain.

Although all Ephrin ligands we studied are influenced in their expression, they differ in their mode of regulation: *ephrin-A5b* is strictly dependent on *ace* function for its expression, whereas both *ephrin-A5a* and *ephrin-A2* depend on *ace* for their graded distribution, but not for expression per se. In mature chick tecta, Engrailed and *ephrin-A5* are coexpressed in glial cells, whereas *ephrin-A2* is expressed in neurons (Millet and Alvarado-Mallart, 1995; Monschau et al., 1997). However, we observe the differences in Ephrin regulation already in the undifferentiated tectum, where these genes are expressed in all tectal cells

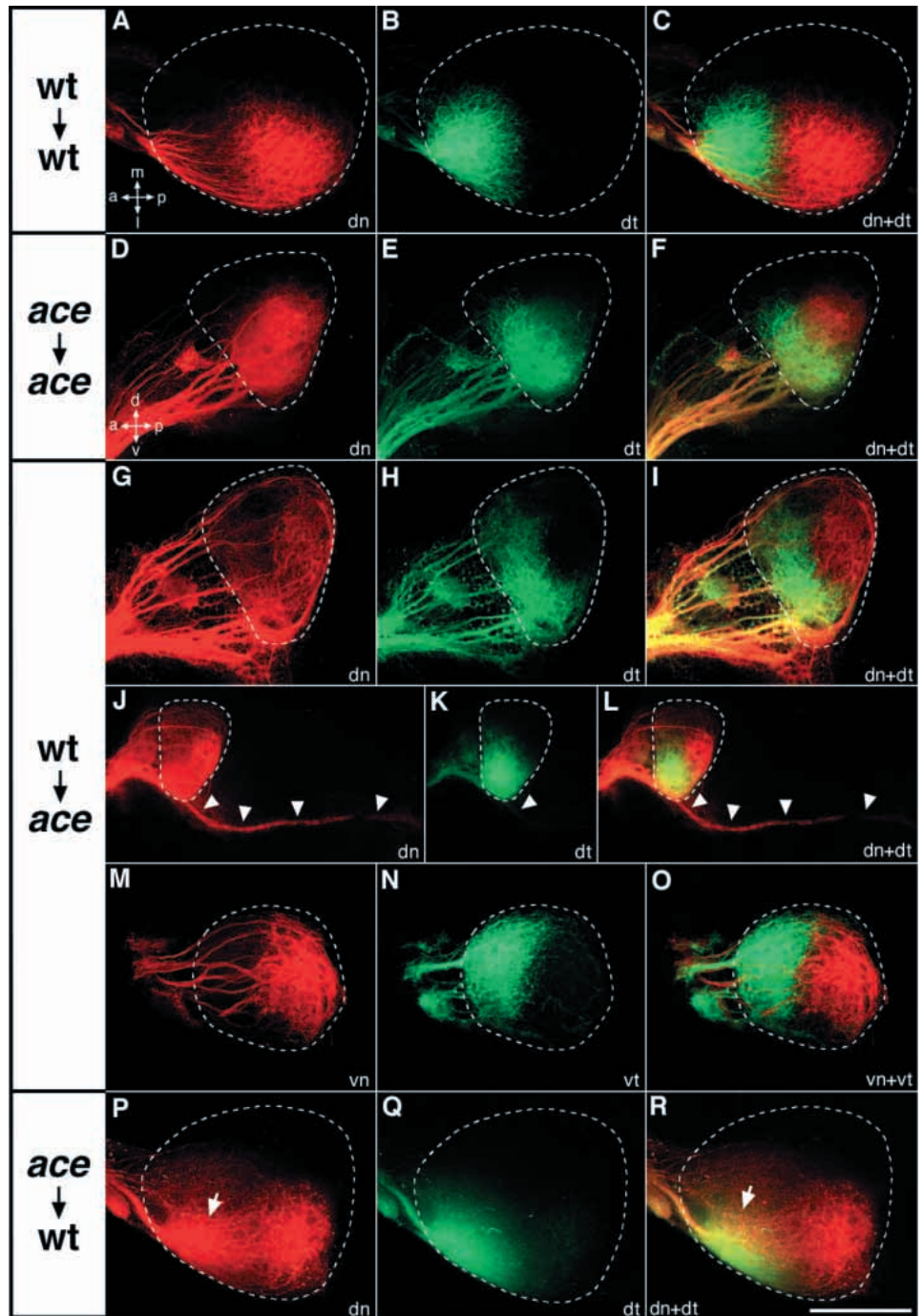


**Fig. 6.** Retinotectal mapping defects in *ace* depend largely on the genotype of the brain. (A-C) Control transplants of wild-type optic vesicles into a wild type host and (D-F) *ace* optic vesicles into *ace* hosts, which reproduce the projection phenotypes of non-manipulated individuals (compare to Fig. 2). (G-O) Chimaeric *ace* hosts with a wild-type optic vesicle graft. Wild-type RGC axon projections on the *ace* mutant tectum are delocalized (G-I) and overshoot posteriorly (J-L, arrowheads) as in *ace* homozygotes. As in *ace* mutants, anterior-posterior mapping on the dorsal tectum is not affected (M-O; dorsal views). (P-R) Chimaeric wild-type host with an *ace* optic vesicle. Dorsotemporal RGC axons from an *ace* eye project normally onto a wild-type optic tectum and do not overshoot, showing that these defects depend on the brain genotype. Note however that dorsonasal RGC axons also terminate inappropriately on the ventroanterior tectal neuropil (arrows), suggesting an autonomous function for Fgf8 in retinal development. A-C and M-R are dorsal views with orientation as indicated in A. D-L are lateral views with orientation as indicated in D. Scale bar, 130  $\mu$ m (J-L) 75  $\mu$ m for all other panels. The tectal neuropil is outlined.

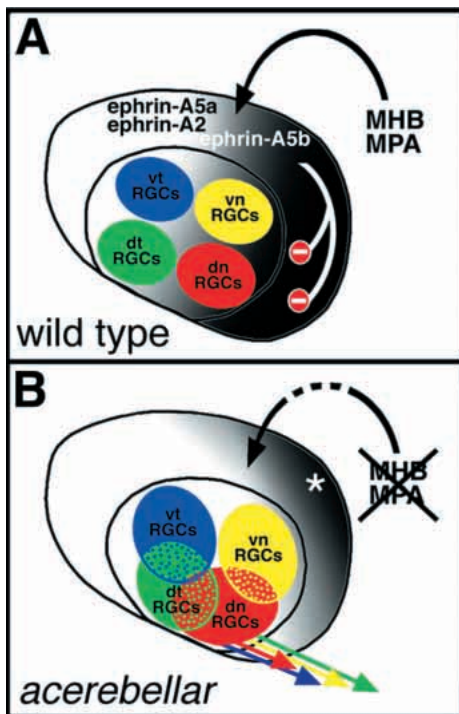


**Fig. 7.** Dual role of the mid-hindbrain boundary in generating tectal polarity and constraining retinal ganglion cell axons to the tectum. In the wild type (A), a midbrain polarizing activity, MPA, from the mid-hindbrain boundary, MHB, is required to maintain (black arrow) an anteriorly to posteriorly increasing graded (white to black shading) expression of the ligands Ephrin-A5a, Ephrin-A2 and Ephrin-A5b. These gradients are necessary for the spatial definition of the tectal termination fields of RGC axons from the four retinal quadrants (coloured circles). In addition, Ephrin-A5b acts as a repellent to restrain RGC axons to the tectum neuropil. Ephrin-A5b is not expressed in *acerebellar* mutants, resulting in loss of a repulsive zone at the posterior tectal margin, which leads to overshooting of axonal projections into the hindbrain. In *acerebellar* mutants (B), the mid-hindbrain boundary is absent due to mutation of *Fgf8*, a candidate component of the MPA. In the absence of the MHB, *ephrin-A5a* and *ephrin-A2* are expressed more evenly, reflecting an anteriorization of the tectum. This leads to a partial delocalization of tectal termination fields, which is particularly evident for dorsal RGCs in the ventral tectum. The signal creating the residual polarity in the *acerebellar* tectum is unknown, but may also determine normal mapping and residual higher Ephrin expression in dorsoposterior levels (asterisk).

(Brennan et al., 1997). Differences in cell type specificity are therefore unlikely to account for the differences in regulation. More likely, the different Ephrins may respond to different levels of *Engrailed*, possibly mediated by different levels of *Fgf8* (see below). In this model, Ephrin A5b would only be activated at the highest *Engrailed* concentrations found in posterior tectum, whereas progressively lower and more anterior *Engrailed* levels would only suffice to activate Ephrin-A5a and Ephrin-A2 in a graded fashion. Gradient formation of Ephrin ligands in the midbrain would depend directly on the anterior-posterior polarization of *Engrailed* expression set during earlier stages in neuroepithelial precursors by a posterior MPA (Fig. 7). We suggest that the MPA is non-functional in *acerebellar* mutants, and tectal

cells thus express Ephrins at levels characteristic for the anterior tectum.

### Repulsive function of the MHB

A second function suggested by our observations is that the MHB prevents RGCs from posterior overshooting into the hindbrain. Overshooting could either be due to an endogenous increased ability of mutant RGC axons to extend, or due to lack of a repulsive activity from the MHB. The fact that overshooting is absent in chimaeras with *ace* RGCs projecting into a wild-type brain argues for a repulsive function of the MHB. Overshooting is seen for all retinal subpopulations, but most frequently for nasal RGCs that normally project to the posterior ventral quadrant of the tectum, close to the site where most overshooting from the tectum takes place. We suggest that axons exit most easily from the tectum at this position, because they can reach alternative axonal tracts which guide them into the hindbrain and beyond. Nasal RGCs may overshoot more frequently in *ace* simply because their normal tectal targets lie closest to the exit point.

Although *Fgf8* from the MHB could itself influence axonal growth (McFarlane et al., 1996), we think it more likely that the repulsive activity is Ephrin-A5b, since (i) it acts *in vitro* to repel axons in chick and zebrafish (Drescher et al., 1995; Brennan et al., 1997) (ii) it shows the most posterior and steepest gradient of expression overlapping the MHB, (iii) it is missing in *ace* mutants, and (iv) mouse embryos lacking Ephrin-A5 show similar overshooting RGC projections (Frisén et al., 1998). We therefore reinforce our previous suggestion (Brennan et al., 1997) that the more posterior localization of *ephrin-A5b* expression, relative to *ephrin-A5a* and *ephrin-A2*, reflects a different function of *ephrin-A5b*, which is to ensure the proper definition of the posterior boundary of the tectal neuropil. In contrast, *Ephrin-A5a* and *Ephrin-A2* might be involved in the relative spatial definition of termination fields.

Together, the findings in mice and zebrafish suggest that the MHB, mediated by Ephrin-A5b, constitutes a repulsive zone for RGC axons that is oriented orthogonally to the midline. The repulsive activity is probably not specific for RGCs, since the trochlear nerve misnavigates in *acerebellar* mutants into the posterior tectal area, which it normally never enters (Fig. 3J,K). We suggest that the same signal may serve to prevent trochlear axons from entering the tectum. Trochlear axons would then be steered by at least two repulsive signals: netrin-dependent repulsion away from the ventral midline would steer the nerve dorsally (Colamarino and Tessier-Lavigne, 1995), while Ephrin-A5b-dependent repulsion would keep the axons on a track orthogonal to the midline. A similar arrangement of repulsive and attractive stripes of tissues that help to keep axons of the postoptic commissure and optic nerve on track has been proposed to exist at the midline surrounding the optic chiasm of the zebrafish (Macdonald et al., 1997).

### Is FGF8 directly involved in polarizing?

The early onset and asymmetric expression relative to the midbrain, and the secreted nature of *Fgf8* protein and phenotypic requirement for *Fgf8* are all consistent with the possibility that *Fgf8* itself might be the posterior MPA, or a component of it. This question cannot at present be decided, however, because in *acerebellar* mutants the MHB does not develop, probably because this tissue is transformed into more

anterior midbrain tissue (Reifers et al., 1998; this paper), which could thus eliminate the true MPA, or other components of it apart from Fgf8. Also, it is unclear whether Fgf8 can diffuse over a sufficient distance to fulfill the function of the MPA. Several additional observations suggest, however, that Fgf8 is the MPA or a component of it. (i) Fgf8 is required to maintain polarized expression of neuroepithelial markers in the midbrain and MHB (Brand et al., 1996; Reifers et al., 1998; Lun and Brand, 1998). (ii) Misexpression of Fgf8 in the dorsal midbrain of mice, chick and zebrafish causes ectopic activation of *Engrailed* and *ephrin-A2* and *-A5* (Lee et al., 1997; Shamim et al., 1999; unpublished observations). (iii) FgfR4, a high-affinity receptor for Fgf8 is present in the tectum (Thisse et al., 1995). (iv) In several tissues, Fgf8 and ephrin family ligands are expressed in close temporal and spatial association. (v) Delocalized Fgf8 expression in mouse embryos lacking the *gbx2* gene, normally expressed in the anterior hindbrain, causes lack of *ephrin-A2* expression in the tectum (Wassarman et al., 1997), although it is not yet known how this affects the retinotectal map.

### Dorsoventral mapping abnormalities

An unexpected finding of our study is that dorsal-ventral polarity of the map and ephrin-A expression is disturbed in *acerebellar* mutants. Dorsal-ventral delocalization is particularly strong for termination fields of nasal RGCs at the posterior tectal margin. Given the in vitro repulsive nature of Ephrin-A5b on axonal growth (Brennan et al., 1997), one possibility is that it acts as a generalized stop signal for axonal growth which itself is not directionally sensitive. In this view, nasal RGCs would continue dorsal-ventral growth along the posterior tectal margin in *ace* because they fail to encounter a signal that generally discourages axon growth. Alternatively, the posterior dorsal-ventral delocalization may reflect a simultaneous alteration of dorsal-ventral positional identities in tectal cells of *ace* mutants. Consistent with this possibility, the extent of ephrin-A ligand expression is reduced not only along the anterior-posterior, but also the dorsal-ventral axis of the tectum, and other, as yet unknown molecules involved in dorsal-ventral mapping may be correspondingly altered. Indeed, we have previously observed transiently altered dorsal-ventral patterning during early somitogenesis stages in *acerebellar* mutants, indicating that patterning along the two axes may be linked (Reifers et al., 1998; Lun and Brand, 1998). The absence of intertectal commissures in *ace* embryos (Fig. 3J,K and unpublished results) that has also been reported after antisense inhibition of *engrailed* expression (Rétaux et al., 1996) may be a reflection of altered dorsal-ventral organisation in the tectum. Further studies of the dorsal-ventral patterning cues for RGC projections, e.g. of EphB receptors and their ligands (Braisted et al., 1997), are required in wild type and in *acerebellar* mutants to distinguish between these possibilities.

Although the map alterations in *acerebellar* mutants are due to changes in overall midbrain polarity, the Ephrin gradients are changed in a coherent way that yields insights into their function. First, our observations agree with previous suggestions that relative, rather than absolute, concentrations of tectal guidance cues are recognized by ingrowing RGC axon growth cones during mapping (Baier and Bonhoeffer, 1994). In the dorsoposterior tectum of *ace* mutants, we find

strongly reduced, albeit still graded expression of ephrin-A ligands at the time of RGC axon ingrowth (Fig. 4). In spite of the low Ephrin levels, RGCs segregate normally along the anterior-posterior axis of the dorsal tectum. This supports the idea that the slope of the gradients in which guidance cues such as the Ephrins are distributed across the tectum governs mapping, rather than absolute protein concentrations. Second, nasal and temporal RGC axons respond in vitro differentially to gradients of Ephrin expression, with temporal axons being repelled by Ephrin-A2 and only weakly by Ephrin-A5 and nasal axons strongly by Ephrin-A5 but not by Ephrin-A2 (Monschau et al., 1997; Brennan et al., 1997). The difference between temporal and nasal RGCs may be due to nasal-temporally different expression levels and/or differences in the phosphorylation status of the Eph receptors on RGCs of the embryonic retina (Connor et al., 1998; Holash and Pasquale, 1995). Our chimaera analysis provides evidence for the in vivo relevance of these differences, since overshooting wild-type RGC axons in an *ace* mutant brain are predominately derived from the nasal retina. This effect is more pronounced in the chimaeras than in *acerebellar* mutants, probably because in the *ace* mutant dorsonasal RGCs are themselves abnormal.

### Development of the optic tract

We have also observed abnormal development of the optic tract in *acerebellar* mutants. In teleosts, RGC axons normally project through the optic tract in order and sort into dorsal and ventral brachia before reaching the tectum (Maggs and Scholes, 1986; Stuermer, 1988). *ace* mutants are variably defective in pathfinding, fasciculation, brachial sorting as well as mapping. Abnormal pathfinding of RGC axons is probably due to forebrain defects that are found particularly in the optic chiasm of the mutants (M. B., S. Shanmugalingam, R. McDonald, A. P., F. R., S. W. Wilson, unpublished observations) which may contribute to the reduced size of the tectal neuropil in *ace* mutants. Alternatively, Fgfs have been suggested to be involved in axonal growth, optic nerve fasciculation and tectal target recognition (Walz et al., 1997; Saffell et al., 1997), and it is possible that some or all of the pathfinding, defasciculation and brachial missorting phenotypes we see reflect this. Previous mistakes along the way to the tectum are, however, unlikely to account for the mapping defects we observe when axons have reached the tectum. In newt and axolotl, RGC axons project topographically correctly even when growing into the tectum via ectopic routes (Fujisawa, 1981; Harris, 1982). Similarly, in the zebrafish mutants *boxer*, *dackel* and *pinscher* brachial sorting is abnormal, but axons are nevertheless correctly targeted in the tectum (Karlstrom et al., 1996; Trowe et al., 1996). Generally, sorting within the optic tract differs widely for different vertebrates, suggesting that its importance for correct mapping is minor (Udin and Fawcett, 1988). Indeed, the brachial missorting of nasal RGCs in *ace* mutants is unlikely to account for their altered dorsal-ventral mapping, since axons entering the tectum through the normal brachium commit the same mapping mistakes as do those entering the tectum via the ectopic brachium. In summary, we believe that the mapping defects we observe are largely due to altered polarized mapping cues on the tectum itself, rather than indirect consequences of abnormal growth trajectories on the way to the tectum.

## Fgf8 and retinal development

The defects we observed in formation of the retinotectal map in *ace* mutants are largely, but not completely restored when *ace* RGCs project into a wild-type brain in chimaeric animals, since dorsonasal RGCs form two foci on a wild-type tectum (Fig. 6P-R); the defect in this RGC subpopulation is less apparent in non-chimaeric *ace* mutants, perhaps due to the simultaneous alteration of tectal guidance cues. Fgf8 is expressed and could therefore function at several stages of retinal development from the early neural plate stage onwards, via the optic vesicle stage, and finally in the retina (Reifers et al., 1998, and unpublished observations). Moreover, retinal patterning is altered by Fgf8 overexpression that occurs in the zebrafish *aussicht* mutant (Heisenberg et al., 1999). It is an intriguing possibility that Fgf8 expression, found on both 'ends' of the visual system, would be available to co-ordinate patterning of retinal ganglion cells and their target field in the midbrain tectum.

We thank our colleagues in the Brand and Holder labs, as well as Uwe Drescher, Suresh Jesuthasan and Torsten Trowe for help with embryo manipulation, discussions and reagents. We are especially indebted to Chi-Bin Chien for teaching us optic vesicle transplantations, and to him and Steve Wilson for comments on the manuscript. We gratefully acknowledge support by grants from the Förderprogramm Neurobiologie Baden-Württemberg, Graduiertenkolleg Neurobiologie and SFB 317 (to M. B.) and from the Wellcome Trust (to N. H.). C. B. was funded by a BBSRC RoPA award to N. H. and S. Wilson.

## REFERENCES

- Baier, H. and Bonhoeffer, F. (1994). Attractive axon guidance molecules. *Science* **265**, 1541-1542.
- Braisted, J. E., McLaughlin, T., Wang, H. U., Friedman, G. C., Anderson, D. J. and O'Leary, D. D. M. (1997). Graded and lamina-specific distributions of ligands of EphB receptor tyrosine kinases in the developing retinotectal system. *Dev. Biol.* **191**, 14-28.
- Brand, M. (1998). Genetic analysis of early development of a vertebrate nervous system in the zebrafish, *Danio rerio*. *Zoology* **101**, 345-364.
- Brand, M. and Granato, M. (1999). Keeping and raising zebrafish. In *Zebrafish: A Practical Approach* (eds. C. Nüsslein-Volhard and S. Schulte-Merker). Oxford: IRL Press.
- Brand, M., Heisenberg, C.-P., Jiang, Y.-J., Beuchle, D., Lun, K., van Eeden, F. J. M., Furutani-Seiki, M., Granato, M., Haffter, P., Hamerschmidt, M. et al. (1996). Mutations in zebrafish genes affecting the formation of the boundary between midbrain and hindbrain. *Development* **123**, 179-190.
- Brennan, C., Monschau, B., Lindberg, R., Guthrie, B., Drescher, U., Bonhoeffer, F. and Holder, N. (1997). Two Eph receptor tyrosine kinase ligands control axon growth and may be involved in the creation of the retinotectal map in the zebrafish. *Development* **124**, 655-664.
- Burrill, J. D. and Easter, S., Jr. (1994). Development of the retinofugal projections in the embryonic and larval zebrafish (*Brachydanio rerio*). *J. Comp. Neurol.* **346**, 583-600.
- Cheng, H. J. and Flanagan, J. G. (1994). Identification and cloning of ELF-1, a developmentally expressed ligand for the Mek4 and Sek receptor tyrosine kinases. *Cell* **79**, 157-168.
- Chung, S. H. and Cooke, J. (1978). Observations on the formation of the brain and of nerve connections following embryonic manipulation of the amphibian neural tube. *Proc. R. Soc. Lond. B Biol. Sci.* **201**, 335-373.
- Colamarino, S. A. and Tessier-Lavigne, M. (1995). The axonal chemoattractant netrin-1 is also a chemorepellent for trochlear motor axons. *Cell* **81**, 621-629.
- Connor, R. J., Menzel, P. and Pasquale, E. B. (1998). Expression and tyrosine phosphorylation of Eph receptors suggest multiple mechanisms in patterning of the visual system. *Dev. Biol.* **193**, 21-35.
- Crossley, P. H. and Martin, G. R. (1995). The mouse Fgf8 gene encodes a family of polypeptides and is expressed in regions that direct outgrowth and patterning in the developing embryo. *Development* **121**, 439-451.
- Crossley, P. H., Martinez, S. and Martin, G. R. (1996). Midbrain development induced by FGF8 in the chick embryo. *Nature* **380**, 66-68.
- Davis, C. A., Holmyard, D. P., Millen, K. J. and Joyner, A. L. (1991). Examining pattern formation in mouse, chicken and frog embryos with an En-specific antiserum. *Development* **111**, 287-298.
- Drescher, U., Kremoser, C., Handwerker, C., Lösinger, J., Noda, M. and Bonhoeffer, F. (1995). In vitro guidance of retinal ganglion cell axons by RAGS, a 25 kDa tectal protein related to ligands for Eph receptor tyrosine kinases. *Cell* **82**, 359-370.
- Flanagan, J. G. and Vanderhaeghen, P. (1998). The ephrins and Eph receptors in neural development. *Annu. Rev. Neurosci.* **21**, 309-345.
- Friedman, G. C. and O'Leary, D. D. (1996). Retroviral misexpression of engrailed genes in the chick optic tectum perturbs the topographic targeting of retinal axons. *J. Neurosci.* **16**, 5498-5509.
- Frisén, J., Yates, P. A., McLaughlin, T., Friedman, G. C., O'Leary, D. D. M. and Barbacid, M. (1998). Ephrin-A5 (AI-1/RAGS) is essential for proper retinal axon guidance and topographic mapping in the mammalian visual system. *Neuron* **20**, 235-243.
- Fujisawa, H. (1981). Retinotopic analysis of fiber pathways in the regenerating retinotectal system of the adult newt *Cynops pyrrhogaster*. *Brain Res.* **206**, 27-37.
- Gardner, C. A. and Barald, K. F. (1991). The cellular environment controls the expression of engrailed-like protein in the cranial neuroepithelium of quail-chick chimeric embryos. *Development* **113**, 1037-1048.
- Harris, W. A. (1980). The effects of eliminating impulse activity on the development of the retinotectal projection in salamanders. *J. Comp. Neurol.* **194**, 303-317.
- Harris, W. A. (1982). The transplantation of eyes to genetically eyeless salamanders: visual projections and somatosensory interactions. *J. Neurosci.* **2**, 339-353.
- Heisenberg, C.-P., Brennan, C. and Wilson, S. W. (1999). Zebrafish *aussicht* mutants exhibit widespread overexpression of *ace(fgf8)* and coincident defects in CNS development. *Development* **126**, 2129-2140.
- Holash, J. A. and Pasquale, E. B. (1995). Polarized expression of the receptor protein tyrosine kinase Cdk5 in the developing avian visual system. *Dev. Biol.* **172**, 683-693.
- Holt, C. E. and Harris, W. A. (1993). Position, guidance, and mapping in the developing visual system. *J. Neurobiol.* **24**, 1400-1422.
- Itasaki, N., Ichijo, H., Hama, C., Matsuno, T. and Nakamura, H. (1991). Establishment of rostrocaudal polarity in tectal primordium: engrailed expression and subsequent tectal polarity. *Development* **113**, 1133-1144.
- Itasaki, N. and Nakamura, H. (1992). Rostrocaudal polarity of the tectum in birds: correlation of en gradient and topographic order in retinotectal projection. *Neuron* **8**, 787-798.
- Joyner, A. L. (1996). Engrailed, Wnt and Pax genes regulate midbrain-hindbrain development. *Trends Genet.* **12**, 15-20.
- Kaethner, R. J. and Stuermer, C. A. (1992). Dynamics of terminal arbor formation and target approach of retinotectal axons in living zebrafish embryos: a time-lapse study of single axons. *J. Neurosci.* **12**, 3257-3271.
- Kaethner, R. J. and Stuermer, C. A. (1994). Growth behavior of retinotectal axons in live zebrafish embryos under TTX-induced neural impulse blockade. *J. Neurobiol.* **25**, 781-796.
- Karlstrom, R. O., Trowe, T., Klostermann, S., Baier, H., Brand, M., Crawford, A. D., Grunewald, B., Haffter, P., Hoffman, H., Meyer, S. U. et al. (1996). Zebrafish mutations affecting retinotectal axon pathfinding. *Development* **123**, 427-438.
- Kimmel, C. B., Ballard, W. W., Kimmel, S. R., Ullmann, B. and Schilling, T. F. (1995). Stages of embryonic development of the zebrafish. *Dev. Dyn.* **203**, 253-310.
- La Vail, M. M. and Hild, W. (1971). Histotypic organization of the rat retina in vitro. *Z. Zellforsch. Mikrosk. Anat.* **114**, 557-579.
- Lee, S. M., Danielian, P. S., Fritschsch, B. and McMahon, A. P. (1997). Evidence that FGF8 signalling from the midbrain-hindbrain junction regulates growth and polarity in the developing midbrain. *Development* **124**, 959-969.
- Logan, C., Wizenmann, A., Drescher, U., Monschau, B., Bonhoeffer, F. and Lumsden, A. (1996). Rostral optic tectum acquires caudal characteristics following ectopic *Engrailed* expression. *Curr. Biol.* **6**, 1006-1014.
- Lumsden, A. and Krumlauf, R. (1996). Patterning the vertebrate neuraxis. *Science* **274**, 1109-1123.
- Lun, K. and Brand, M. (1998). A series of *no isthmus (noi)* alleles of the

- zebrafish *pax2.1* gene reveals multiple signaling events in development of the midbrain-hindbrain boundary. *Development* **125**, 3049-3062.
- Macdonald, R., Scholes, J., Strähle, U., Brennan, C., Holder, N., Brand, M. and Wilson, S. W.** (1997). The Pax protein *Noi* is required for commissural axon pathway formation in the rostral forebrain. *Development* **124**, 2397-2408.
- Maggs, A. and Scholes, J.** (1986). Glial domains and nerve fiber patterns in the fish retinotectal pathway. *J. Neurosci.* **6**, 424-438.
- Martinez, S. and Alvarado-Mallart, R. M.** (1990). Expression of the homeobox *Chick-en* gene in chick/quail chimeras with inverted mesencephalic grafts. *Dev. Biol.* **139**, 432-436.
- Martinez, S., Wassef, M. and Alvarado-Mallart, R. M.** (1991). Induction of a mesencephalic phenotype in the 2-day-old chick prosencephalon is preceded by the early expression of the homeobox gene *en*. *Neuron* **6**, 971-981.
- McFarlane, S., Cornel, E., Amaya, E. and Holt, C. E.** (1996). Inhibition of FGF receptor activity in retinal ganglion cell axons causes errors in target recognition. *Neuron* **17**, 245-254.
- Millen, K. J., Wurst, W., Herrup, K. and Joyner, A.** (1994). Abnormal embryonic cerebellar development and patterning of postnatal foliation in two mouse *Engrailed-2* mutants. *Development* **120**, 695-706.
- Millet, S. and Alvarado-Mallart, R. M.** (1995). Expression of the homeobox-containing gene *En-2* during the development of the chick central nervous system. *Eur. J. Neurosci.* **7**, 777-791.
- Monschau, B., Kremoser, C., Ohta, K., Tanaka, H., Kaneko, T., Yamada, T., Handwerker, C., Hornberger, M. R., Lösinger, J., Pasquale, E. B. et al.** (1997). Shared and distinct functions of RAGS and ELF-1 in guiding retinal axons. *EMBO J.* **16**, 1258-1267.
- Nakamura, H., Itasaki, N. and Matsuno, T.** (1994). Rostrocaudal polarity formation of chick optic tectum. *Int. J. Dev. Biol.* **38**, 281-286.
- O'Leary, D. D. M., Yates, P. A. and McLaughlin, T.** (1999). Molecular development of sensory maps: representing sights and smells in the brain. *Cell* **96**, 255-269.
- Orioli, D. and Klein, R.** (1997). The Eph receptor family: axonal guidance by contact repulsion. *Trends Genet.* **13**, 354-359.
- Postlethwait, J. H., Yan, Y. L., Gates, M. A., Horne, S., Amores, A., Brownlie, A., Donovan, A., Egan, E. S., Force, A., Gong, Z. et al.** (1998). Vertebrate genome evolution and the zebrafish gene map. *Nature Genet.* **18**, 345-349.
- Reifers, F., Böhli, H., Walsh, E. C., Crossley, P. H., Stainier, D. Y. R. and Brand, M.** (1998). *Fgf8* is mutated in zebrafish *acerebellar* mutants and is required for maintenance of midbrain-hindbrain boundary development and somitogenesis. *Development* **125**, 2381-2395.
- Rétaux, S. and Harris, W. A.** (1996). Engrailed and retinotectal topography. *Trends Neurosci.* **19**, 542-546.
- Rétaux, S., McNeill, L. and Harris, W. A.** (1996). Engrailed, retinotectal targeting, and axonal patterning in the midbrain during *Xenopus* development: an antisense study. *Neuron* **16**, 63-75.
- Saffell, J. L., Williams, E. J., Mason, I. J., Walsh, F. S. and Doherty, P.** (1997). Expression of a dominant negative FGF receptor inhibits axonal growth and FGF receptor phosphorylation stimulated by CAMs. *Neuron* **18**, 231-242.
- Shamim, H., Mahmood, R., Logan, C., Doherty, P., Lumsden, A. and Mason, I.** (1999). Sequential roles for *Fgf4*, *En1* and *Fgf8* in specification and regionalisation of the midbrain. *Development* **126**, 945-959.
- Stuermer, C. A. O.** (1988). Retinotopic organization of the developing retinotectal projection in the zebrafish embryo. *J. Neurosci.* **8**, 4513-4530.
- Stuermer, C. A., Rohrer, B. and Munz, H.** (1990). Development of the retinotectal projection in zebrafish embryos under TTX-induced neural-impulse blockade. *J. Neurosci.* **10**, 3615-3626.
- Thisse, B., Thisse, C. and Weston, J. A.** (1995). Novel FGF receptor (*Z-FGFR4*) is dynamically expressed in mesoderm and neurectoderm during early zebrafish embryogenesis. *Dev. Dyn.* **203**, 377-391.
- Trowe, T., Klostermann, S., Baier, H., Grunewald, B., Hoffmann, H., Karlstrom, R. O., Granato, M., Haffter, P., Hammerschmidt, M., van Eeden, F. J. M. et al.** (1996). Mutations disrupting the ordering and topographic mapping of axons in the retinotectal projection of the zebrafish, *Danio rerio*. *Development* **123**, 439-450.
- Udin, S. B. and Fawcett, J. W.** (1988). Formation of topographic maps. *Annu. Rev. Neurosci.* **11**, 289-327.
- Walter, J., Kern-Veits, B., Huf, J., Stolze, B. and Bonhoeffer, F.** (1987). Recognition of position-specific properties of tectal cell membranes by retinal axons *in vitro*. *Development* **101**, 685-696.
- Walz, A., McFarlane, S., Brickman, Y. G., Nurcombe, V., Bartlett, P. F. and Holt, C. E.** (1997). Essential role of heparan sulfates in axon navigation and targeting in the developing visual system. *Development* **124**, 2421-2430.
- Wassarman, K. M., Lewandoski, M., Campbell, K., Joyner, A. L., Rubenstein, J. L., Martinez, S. and Martin, G. R.** (1997). Specification of the anterior hindbrain and establishment of a normal mid/hindbrain organizer is dependent on *Gbx2* gene function. *Development* **124**, 2923-2934.
- Westerfield, M.** (1994). *The Zebrafish Book*. Edition 2.1, Oregon: University of Oregon Press.
- Wurst, W., Auerbach, A. B. and Joyner, A. L.** (1994). Multiple developmental defects in *Engrailed-1* mutant mice: an early mid-hindbrain deletion and patterning defects in forelimbs and sternum. *Development* **120**, 2065-2075.
- Xu, Q., Holder, N., Patient, R. and Wilson, S. W.** (1994). Spatially regulated expression of three receptor tyrosine kinase genes during gastrulation in the zebrafish. *Development* **120**, 287-299.